Entergy Nuclear Operations, Inc.
Pilgrim Nuclear Power Station
600 Rocky Hill Road
Plymouth, MA 02360

July 22, 2016

U.S. Nuclear Regulatory Commission
Attn: Document Control Desk
Washington, DC 20555-0001

SUBJECT: Pilgrim Nuclear Power Station - Information Needs for the Flooding Hazard Reevaluation Report; Storm Surge Analysis

Pilgrim Nuclear Power Station
Docket No. 50-293
Renewed License No. DPR-35

LETTER NUMBER: 2.16.043

Dear Sir or Madam:

Per request from a U.S. NRC Senior Project Manager; Japan Lessons Learned Division, Pilgrim Nuclear Power Station (PNPS) is submitting the responses to the five Information Needs for the Flooding Hazard Reevaluation Report; Storm Surge Analysis. These responses were the primary focus of a Webinar between the NRC Staff and PNPS on June 16, 2016 initiated by Mr. Victor Hall (Senior Project Manager, Japan Lessons Learned Division).

If you have any questions or require additional information, please contact me at (508) 830-8323.

There are no regulatory commitments contained in this letter.

Sincerely,

Everett P. Perkins, Jr.
Manager, Regulatory Assurance
EPP/rb

Attachment: Pilgrim Nuclear Power Station - Information Needs for the Flooding Hazard Reevaluation Report; Storm Surge Analysis (33 Pages)

A001
NRR

cc: Mr. Daniel H. Dorman
Regional Administrator, Region I
U.S. Nuclear Regulatory Commission
2100 Renaissance Boulevard, Suite 100
King of Prussia, PA 19406-2713

Ms. Booma Venkataraman, Project Manager
Office of Nuclear Reactor Regulation
U.S. Nuclear Regulatory Commission
Mail Stop O-8C2A
Washington, DC 20555

Mr. Victor Hall, Senior Project Manager
Japan Lessons Learned Division
Office of Nuclear Reactor Regulation
U.S. Nuclear Regulatory Commission
Mail Stop 13 C5
Washington, DC 20555

NRC Senior Resident Inspector
Pilgrim Nuclear Power Station

ATTACHMENT

Letter Number 2.16.043

Pilgrim Nuclear Power Station

Information Needs for the Flooding Hazard Reevaluation Report; Storm Surge Analysis

(33 Pages)

Pilgrim Nuclear Power Station (PNPS)
Information Needs for the Flood Hazard Reevaluation Report
Storm Surge Analysis

Information Need 1: Storm Surge Analysis – Storm Selection

Background: Section 3.4.1.1 of the Flood Hazard Reevaluation Report (FHRR) provides a discussion of the Probable Maximum Hurricane (PMH) and Probable Maximum Winds Storm development. The evaluation of the PMH includes synthetic hurricane data representative of a large set of synthetic tropical cyclone tracks. The FHRR states the synthetic data were developed by Dr. Kerry Emanuel of WindRiskTech, LLC using coupled intensity and atmospheric models (FHRR cites AREVA 2015a). The methodology used to develop the synthetic tropical cyclone tracks and storm parameters includes: 1) storm generation; 2) storm track generation; and 3) deterministic modeling of hurricane intensity. Using this methodology, a large number (i.e., 10,013) of synthetic storm tracks (i.e., referred to herein as the WRT storm set) was generated and filtered within a radius of 200 kilometers (km) of Plymouth, Massachusetts (MA) to support the evaluation of the PMH at PNPS.

The Emanuel model applied to generate the synthetic storms in this study provides a state-of-the-art tool. However, the treatment of coastal effects on storms is not well developed and the contribution of baroclinic energy sources appears to be neglected in this model. The transition from a purely latent heat source storm to a hybrid storm, with important contributions from both latent heat and baroclinic sources is not uncommon at latitudes near PNPS. Weather maps of Sandy and the 1938 hurricane both depict fronts imbedded within the storm during their approach to the coast.

Reference: AREVA, 2015a. AREVA Document No. 32-9226726-000. Pilgrim Nuclear Power Station Flooding Hazard Re-Evaluation – Probable Maximum Hurricane/ Probable Maximum Wind Storm. 2015.

Request: Discuss how the Emanuel model considers baroclinic energy sources. If baroclinic energy sources are not included, discuss the implications on the PMH parameters derived from the Emanuel model results.

Response:

The Emanuel model does not attempt to explicitly represent baroclinic energy sources that contribute to the potential re-intensification of cyclones during or after extratropical transition (ET). However, the model does include the impact of enhanced forward motion often associated with ET on a hurricane's maximum wind speed, as it accounts for stronger steering currents that occur at the latitudes at which ET typically occurs. It also permits a major hurricane to move more rapidly into the New England area such that the dissipation of the storm due to the loss of its tropical energy sources does not occur as quickly as it does for a slower moving storm. For major hurricanes, the factors described above are more likely to influence the maximum wind speed of a PMH in the PNPS area relative to an explicit representation of intensification due to baroclinic energy conversions. These considerations support the conclusion that the PMH parameters presented in the FHRR are adequately conservative for the PNPS study area.

Please refer to **Appendix A** for a more detailed discussion of this topic.

Information Need 2: Storm Surge Analysis – Storm Selection

Background: Table 3-5 of the FHRR provides the recommended PMH parameters for PNPS, based on the FHRR site-specific meteorology study. The table shows decreasing maximum wind speeds as storms head more west of north. Because the FHRR analysis occurs in a region where tropical cyclones can move fast (mostly retaining their intensity), and because storms can loop west after staying over homogenous water temperature in this region, it's not clear that the FHRR's lower central pressure values at more westward motions adequately define the PMH.

Request: Provide additional justification that the FHRR's lower central pressure values at more westward motions adequately define the PMH for the degree of storm intensity.

Response:

A site-and-region-specific hurricane meteorology study was conducted to support the PMH calculation at PNPS assessed historical and synthetic hurricane data. Detailed statistical analyses were performed to characterize correlations amongst parameters within each data set and to determine similarity between the data sets. Parameter combinations subject to assessment included storm intensity (i.e., measured via maximum wind speed) and storm direction (i.e., referred to as bearing measured clockwise relative to north). Please refer to **Appendix B**, which summarizes findings relative to the correlation between intensity and storm bearing, as extracted from the PNPS calculation (AREVA, 2015a). These findings highlight the distinct characteristic of reduced maximum wind speeds for storms with more westerly motions within the study area and provide appropriate justification for representation of such a relationship in describing the PMH at PNPS.

Note: correlations amongst parameter pairings were generally non-linear; therefore, linear regressions shown in figures within **Appendix B** are for reference only and should not be used to assess similarities or differences between data sets.

Reference: AREVA, 2015a. AREVA Document No. 32-9226726-000. Pilgrim Nuclear Power Station Flooding Hazard Re-Evaluation – Probable Maximum Hurricane/ Probable Maximum Wind Storm. 2015.

Information Need 3: Storm Surge Analysis – Stillwater and Wave Runup Values

Background: Table 4-4 of the FHRR provides the Current Licensing Basis (CLB) flood hazard and re-evaluated flood hazard values for several flood scenario parameters. Table 4-4 lists an elevation of 22.1 ft-MSL for both the maximum stillwater elevation and the maximum wave runup elevation. Based on the information provided in Table 4-4, the staff understands that wave runup for the Storm Surge Flooding Hazard is 0.0 ft.

Request: Provide an analysis and discussion for selecting this wave runup value.

Response:

The following table provides clarification with respect to how the re-evaluated flood hazard elevation was calculated for the Combined Effect Flood at PNPS:

Combined Effect Flood

Location	Stillwater Elevation	Wave Runup Height / Reflected Wave Height	Re-Evaluated Flood Hazard
Near Reactor Building in site yard between buildings and shore revetment	15.8 feet MSL	6.3 feet	22.1 feet MSL
Upstream face of Intake Structure	15.8 feet MSL	4.0 feet	19.8 feet MSL

Presented below is a modified version of Table 4-4 from the PNPS FHRR that is consistent with the clarifications provided above (AREVA, 2015b). Modifications to this table are shown in red text. Please note: these modifications were presented previously in response to Information Needs related to the Local Intense Precipitation (LIP) analysis at PNPS.

Excerpt from Table 4-4 (AREVA, 2015b): Combined Effect Flood

Flood Scenario Parameter		CLB Flood Hazard	Re-Evaluated Flood Hazard	Re-Evaluated Flood Hazard Information Source	Bounded (B) or Not Bounded (NB)
Flood Level and Associated Effects	Max. Still Water Elevation	Not identified in the CLB.	22.1 feet MSL (near Reactor Building in site yard between buildings and shore revetment). This number (i.e., 22.1 feet MSL) represents combined conditions of the maximum stillwater and wave setup elevation of 15.8 feet MSL plus wave runup on the shoreline revetment. 19.8 feet MSL (upstream face of Intake Structure).	Derived from combined effects flooding hazard analysis (AREVA, 2015b).	NB (See Section 5.0)

Flood Scenario Parameter		CLB Flood Hazard	Re-Evaluated Flood Hazard	**Re-Evaluated Flood Hazard Information Source**	Bounded (B) or Not Bounded (NB)
			This number (i.e., 19.8 feet MSL) represents combined conditions of the maximum stillwater and wave setup elevation of 15.8 feet MSL plus the reflected wave crest height at the intake structure. [Note: Station grade is at 20 feet MSL]		
Note: B/NB indicates if the re-evaluation parameters or results are bounded/not bounded by the CLB evaluation parameters or results.					

Reference: AREVA, 2015b, AREVA Document No. 51-9226940-000. Pilgrim Nuclear Power Station Flooding Hazard Re-Evaluation Report. 2015.

Information Need 4: Storm Surge Analysis - Wave Modeling and Total Water Levels

Background: Section 2.4 of the FHRR points out that the PNPS breakwaters were damaged during winter storms in 1977-1978 and 1978-1979. The FHRR states the breakwaters were repaired to the original configuration and are now monitored annually. The FHRR does not indicate the breakwaters were made more robust. Therefore, the PMH event, which will have higher water levels and forcing than the winter storms of 1977-1978 and 1978-1979, could cause damage to the breakwaters and reduce their effectiveness in reducing wave heights near PNPS.

Also, based on Figure 3-46, the staff have noted that westerly directed waves could enter breakwater opening, which could lead to larger wave heights and potentially increased wave runup and total water levels at PNPS.

Request:

a. Discuss how the breakwaters were applied within the SWAN subgrid wave modeling, including if the prior damage to the breakwaters (winter storms of 1977-1978 and 1978-1979) was considered and included in the model setup. If the breakwaters were

considered as fixed and robust structures within the SWAN subgrid wave modeling, discuss the implications of how damage to the breakwaters during actual storms may increase the wave energy that reaches the revetment near PNPS and total water level near the PNPS infrastructure.

b. Discuss if any PMH simulations resulted in more westerly-directed waves that produced larger wave heights propagating through the breakwater opening and impacting the PNPS revetment.

Response – Part a:

The breakwaters were represented in the nearshore SWAN model as fixed and robust structures in a manner consistent with current site conditions. In reference to flooding levels presented in the FHRR, the applied model did not dynamically estimate and/or represent damage that might occur during the PMH or PMWS simulations that would have modified the breakwaters from their initial/existing conditions. As indicated above, these structures did experience localized and relatively minor damage during two severe coastal winter storms occurring during the late 1970s, which ultimately resulted in repairs and implementation of a monitoring program to periodically assess integrity and functionality.

While it is important to note that damage was not widespread despite near-optimal damage-causing potential (i.e., long-duration, high-intensity wave conditions over multiple tidal cycles) during these storms, it is reasonable to assume that it is possible that the PMH or PMWS may result in some degree of damage to the breakwaters.

To assess these potential effects, a sensitivity analysis was performed using the nearshore SWAN model. Damage estimates, in the form of percent reductions to the top elevation of the main breakwater, were developed based on the Hudson formula, which is commonly applied in designing breakwaters and/or assessing damaging wave conditions (USACE, 1995). **Appendix C** details calculations that produced estimated potential percent damages of approximately 9% during the PMH and approximately 18% during the PMWS based on maximum simulated significant wave heights during each event. Based on the PMWS damage estimate, a variation of the original SWAN model bathymetry was designed to conservatively reflect a reduction of 20% to the top elevation of the main breakwater at the outset of simulated time (i.e., the model bathymetry is modified prior to PMH or PMWS occurrence). Simulations, subject to a number of conservative assumptions (i.e., as described below), were then performed using the nearshore SWAN model reflective of the reduced breakwater elevation for the PMH and PMWS cases. Wave characteristics were then extracted and used to estimate wave runup elevations and maximum water surface elevations for the transects shown in the following figure under each simulated condition:

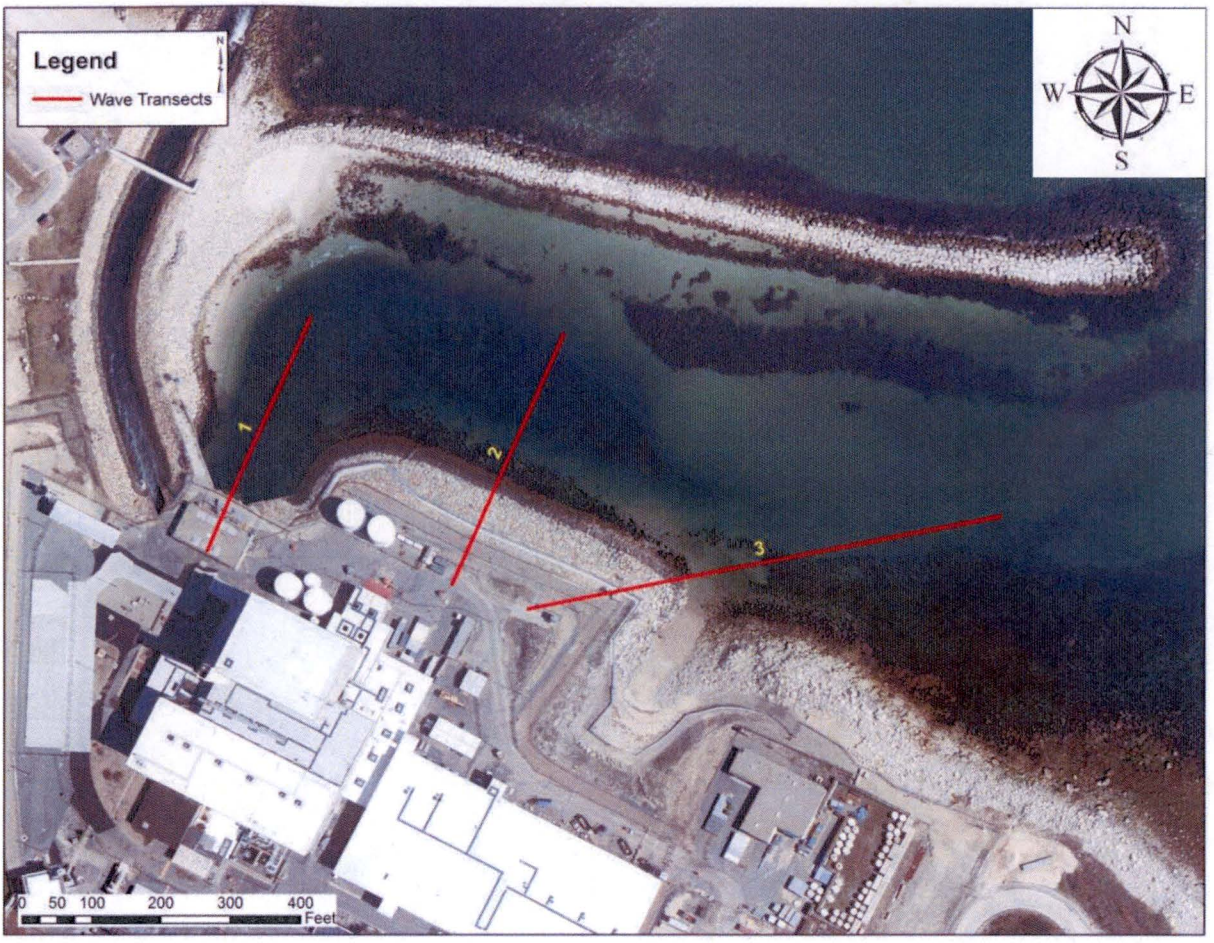

Figure 15 from AREVA, 2015b: PNPS Wave Transects

The resulting wave effect calculations are summarized below for Transects 1, 2, and 3, respectively. It is important to note that the values presented in these tables represent final re-evaluated total water surface or adjusted wave runup elevations that include consideration of storm-induced surge, wave setup, and wave runup. Furthermore, it is important to note that the simulated damage scenario is considered to be a very conservative representation of maximum potential damage to the main breakwater, as the damage estimate was based on several conservative assumptions including, but not limited to, the following:

- Damage potential was conservatively assessed using the maximum simulated wave height for the PMH and PMWS scenarios without consideration of the specific timing of the condition. Based on examination of time series extracted for the PMH scenario, maximum simulated wave conditions occur approximately 8 hours after the main breakwater is submerged. It is important to note that physical modeling performed in support of the original design of the breakwater structures suggested damage potential was greatest when stillwater levels reached 2 feet below the structure crest elevation (i.e., stillwater elevation approximately 8.5 feet NAVD88).

- While damage estimates for the PMH and PMWS differed due to different maximum wave conditions, model simulations were performed for a single damage condition reflective of a condition at the upper limit of the category associated with the maximum estimated damage (i.e., 20% damage associated with the PMWS estimate of 18%). This approach is conservative overall but particularly so relative to the PMH scenario, as the damage estimate was approximately 9%.

- Model simulations reflective of a damaged main breakwater structure were performed assuming damage was complete and present prior to the arrival of the PMH or PMWS. This approach is conservative in both cases, but it is particularly conservative with respect to the PMH, as this event has a relatively short duration.

Transect 1 - Intake

PMH **T1 - Intake - Node 12**	
FHRR - Zero Breakwater Damage	20% Reduction Breakwater
Total WSE, ft MSL	Total WSE, ft MSL
19.8	20.5

PMWS **T1 - Intake - Node 12**	
FHRR - Zero Breakwater Damage	20% Reduction Breakwater
Total WSE, ft MSL	Total WSE, ft MSL
18.7	19.6

Note: Total WSE indicates total water surface elevation at the PNPS intake.

Transect 2 – Reactor Building

PMH T2 - Reactor Building - Node 15			
FHRR - Zero Breakwater Damage		20% Reduction Breakwater	
Inland Limit, ft	Ra, ft MSL	Inland Limit, ft	Ra, ft MSL
81	21.9	107	22.3

PMWS T2 - Reactor Building - Node 15			
FHRR - Zero Breakwater Damage		20% Reduction Breakwater	
Inland Limit, ft	Ra, ft MSL	Inland Limit, ft	Ra, ft MSL
70	21.7	84	21.9

Transect 3 – Boat Ramp

PMH T3 - Boat Ramp - Node 20			
FHRR - Zero Breakwater Damage		20% Reduction Breakwater	
Inland Limit, ft	Ra, ft MSL	Inland Limit, ft	Ra, ft MSL
153	22.1	160	22.2

PMWs T3 - Boat Ramp - Node 20			
FHRR - Zero Breakwater Damage		20% Reduction Breakwater	
Inland Limit, ft	Ra, ft MSL	Inland Limit, ft	Ra, ft MSL
180	22.4	189*	22.5

Notes: *indicates estimate based on extrapolation of the applied relationship between maximum wave height and inland limit of runup from bluff crest (FEMA, 2007).

As indicated by the information provided above, the conservative breakwater damage scenario assessed as part of the sensitivity analysis did not result in a total water surface elevation above 21.5 ft MSL at the PNPS intake or a wave runup condition exceeding an elevation of 23.0 ft MSL, the critical elevation.

References:

AREVA, 2015b. AREVA Document No. 51-9226940-000. Pilgrim Nuclear Power Station Flooding Hazard Re-Evaluation Report. 2015.

FEMA, 2007. "Atlantic Ocean and Gulf of Mexico Coastal Guidelines Update", Federal Emergency Management Agency, February 2007.

USACE, 1995. Design of Coastal Revetments, Seawalls, and Bulkheads. EM 1110-2-1614.

Response – Part b:

A detailed analysis focusing on optimally aligning wave approach angles with the breakwater opening was not specifically performed in support of the FHRR; however, as indicated by Figures 3.9-11 and 3.9-12 from the PNPS FHRR, which are reproduced below, wave directions associated with peak wave conditions occurring during the PMH and PMWS are aligned with the opening of the breakwater pairing at PNPS. Thus, wave conditions (i.e., wave height and period) used to perform runup calculations do consider some bypassing behavior. While these figures clearly show peak wave conditions striking the shoreline at oblique angles, runup calculations were performed assuming head-on wave alignment. This very conservative assumption maximizes runup at all assessed locations above the maximum predicted stillwater elevations generated by the PMH and PMWS, respectively. This conservative approach would offset any slight increase in wave conditions resulting from storm alignment modification, which would also result in a reduced stillwater elevation relative to the PMH or PMWS.

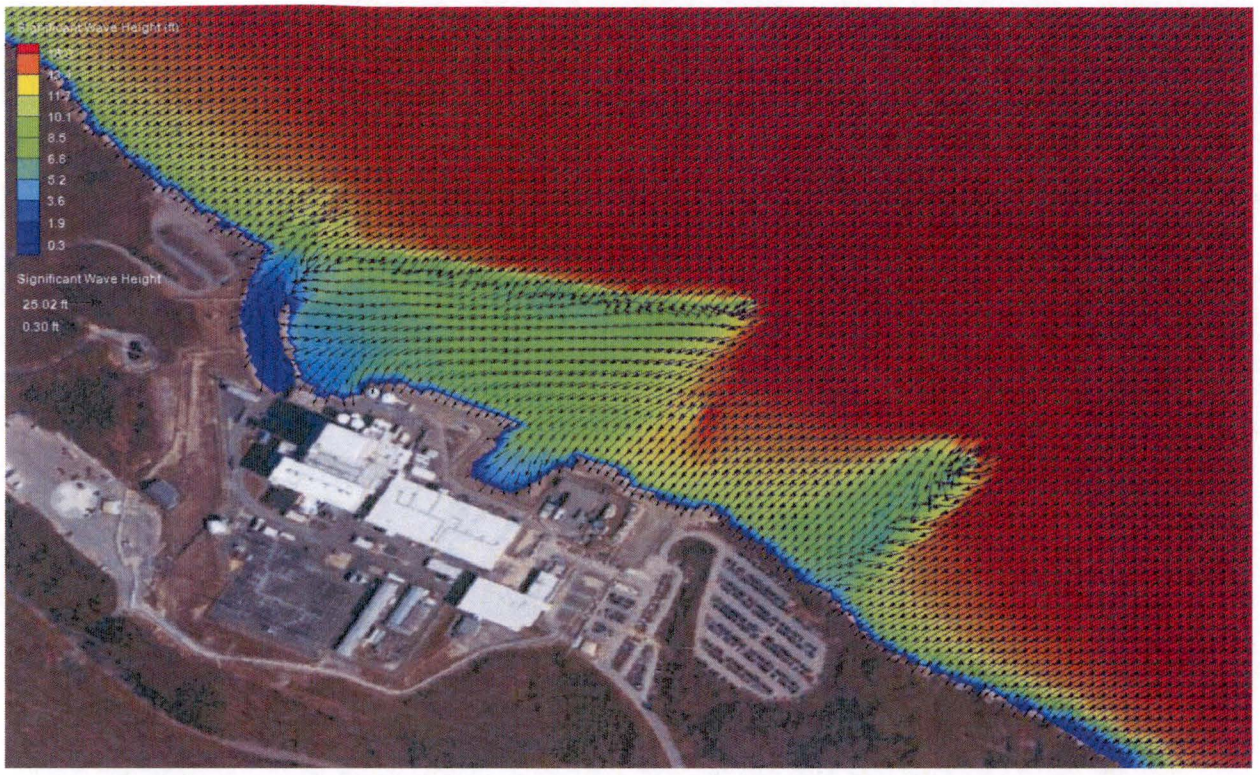

Figure 3.9-11 from AREVA, 2015b: Peak Significant Wave Height - PMH

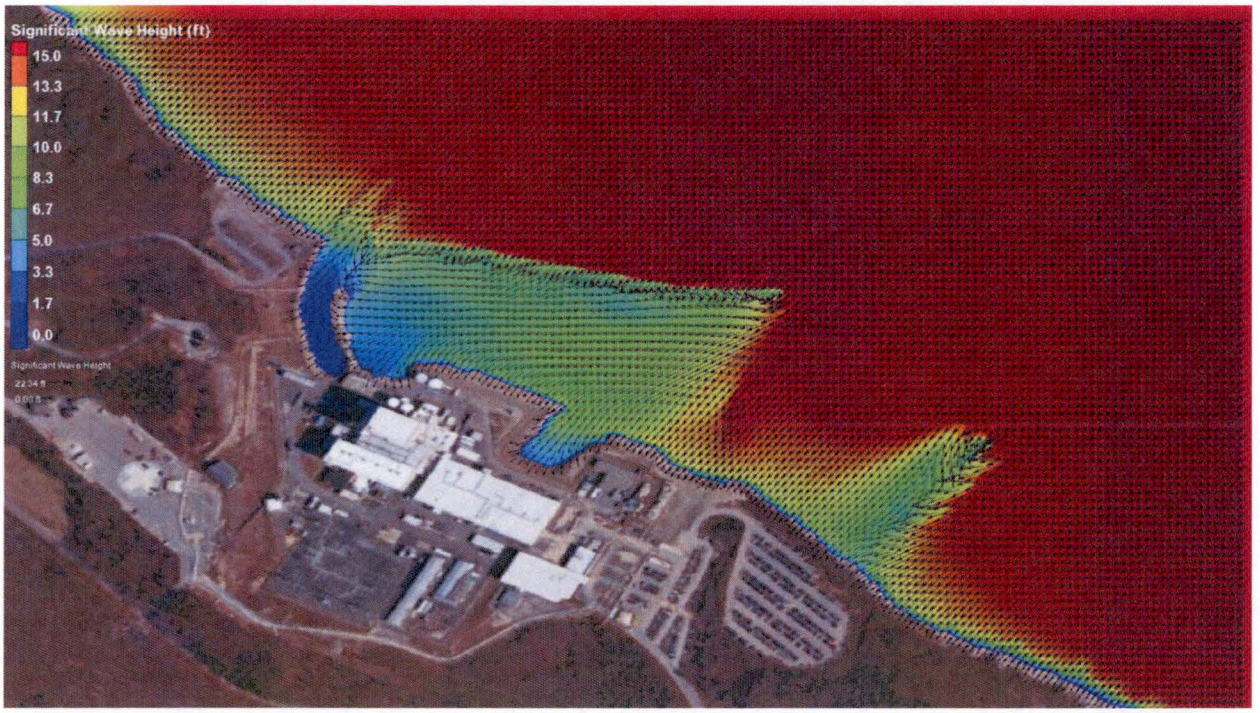

Figure 3.9-12 from AREVA, 2015b: Peak Significant Wave Height – PMWS

Reference: AREVA, 2015b. AREVA Document No. 51-9226940-000. Pilgrim Nuclear Power Station Flooding Hazard Re-Evaluation Report. 2015

Information Need 5: Storm Surge Analysis – Wave Modeling and Total Water Levels

Background: Independent SWAN+ADCIRC model simulations with NRC staff-developed storm parameters showed the wave induced water level change (wave setup) was more pronounced for storms heading west of north. Table 3-8 of the FHRR only shows results from one simulation, so any variation in wave setup across the candidate PMH storms cannot be assessed.

Section 3.4.2.2.3 of the FHRR discusses additional evaluations of flooding potential and wave runup effects performed using a high-resolution nearshore wave modeling. However, Section 3.9 does not provide results from the high-resolution nearshore wave modeling.

Request: Discuss any FHRR PMH candidate simulations that resulted in larger wave setup values than the PMH storm results in Table 3-8. Discuss the high-resolution nearshore wave modeling (FHRR Section 3.9) and the estimates of wave setup near PNPS using this model. Also, discuss the effects of larger wave setup on the wave runup and the total water surface elevation at PNPS site.

Response:

The influence of wave setup on maximum stillwater elevations at PNPS was initially assessed using the difference between PMH candidate simulations performed using ADCIRC and SWAN+ADCIRC (i.e,. the former excluding wave setup in maximum stillwater elevation output, and the latter including wave setup in maximum stillwater elevation output). As shown in the figure below, the controlling PMH scenario (i.e., STORMID 3397 at a bearing of 10 degrees) resulted in the maximum stillwater condition with only a slight difference in wave setup magnitude relative to the other PMH candidates. In agreement with the statement presented above, wave setup magnitude was determined to be increasing slightly in simulations associated with PMH candidates moving more west-of-north; however, maximum stillwater elevation, which included wave setup via SWAN+ADCIRC, was selected as the governing criterion for identifying the PMH subject to site-scale runup calculations.

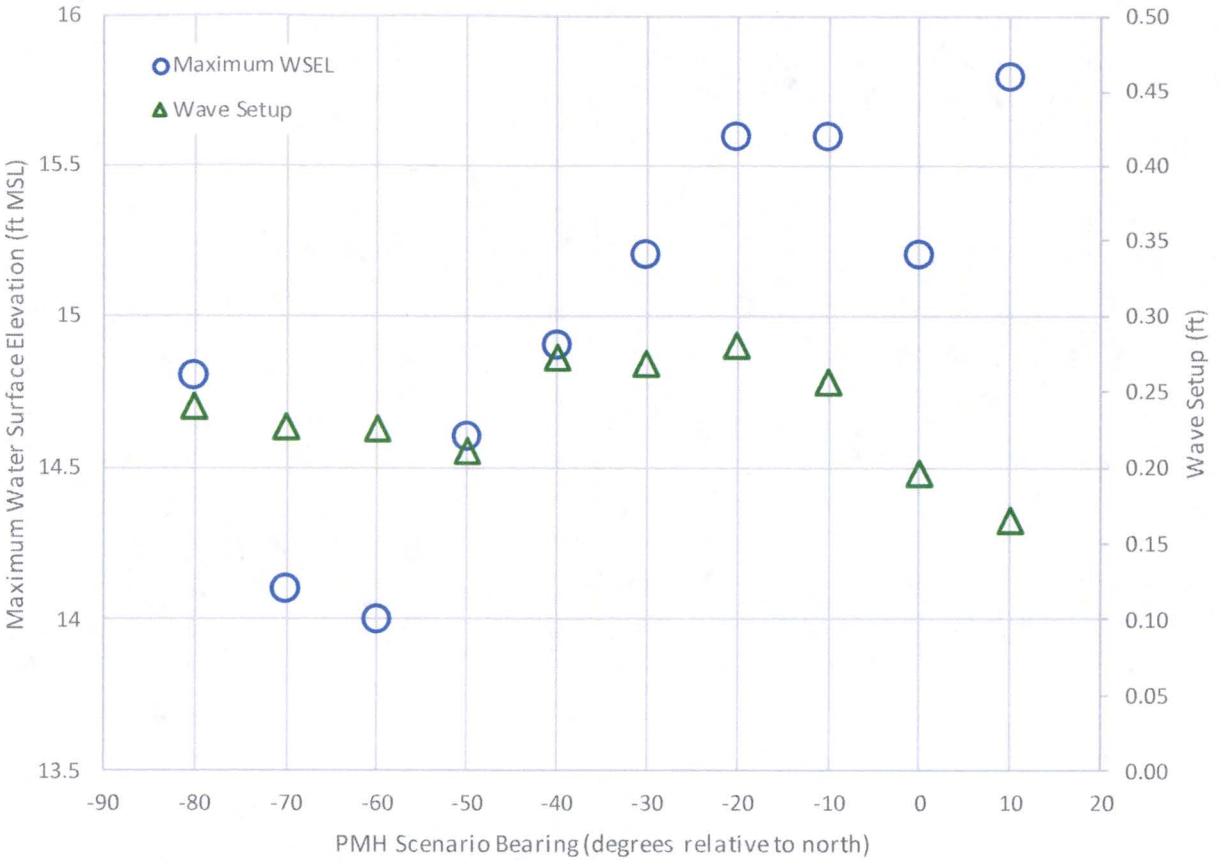

Note: maximum water surface elevation (WSEL) reflects stillwater plus wave setup, as simulated via the SWAN+ADCIRC model.

Site-scale wave effect analyses were supported by output obtained from PMH and PMWS simulations performed using a finer-resolution SWAN model (i.e., relative to the resolution of the SWAN+ADCIRC mesh). The SWAN model was used to simulate the nearshore and shallow-water wave action in the immediate vicinity of PNPS. A separate SWAN model was necessary to resolve the topography and detailed bathymetry, which includes the breakwater structures, present in the PNPS site area. Because of these features, the separate SWAN model was judged to be portray nearshore conditions, particularly inside the breakwater.

In developing the nearshore SWAN model, an irregular mesh (i.e., not a rectilinear grid) was used to represent site-specific geometry with detail. While this approach prevented direct output of wave setup values, checks were performed to determine similarity in wave conditions. The results of these checks, which resulted in only minor observable differences, are summarized below.

Table 6 from AREVA, 2015c: Deep water and Nearshore/Shallow-Water Model Comparison – PMH

Point		Offshore coupled SWAN+ADCIRC Model	Nearshore/Shallow-Water SWAN Model	Difference (Offshore - Nearshore)	Percent Difference
V1	Peak Significant Wave Height (feet)	21.6	20.3	1.3	6.2
	Peak Wave Period (seconds)	10.5	11.0	-0.5	4.7
V2	Peak Significant Wave Height (feet)	18.4	17.4	1.0	5.5
	Peak Wave Period (seconds)	10.9	9.8	1.1	10.6

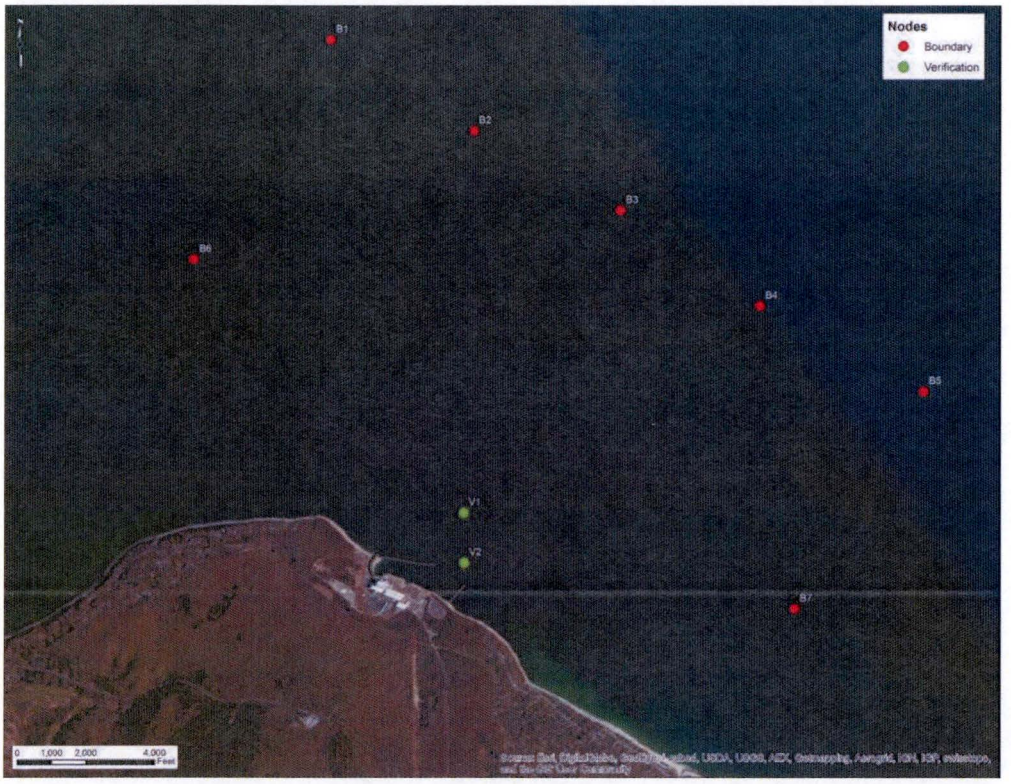

Figure 10 from AREVA, 2015c: Coupled SWAN+ADCIRC Simulation Output Locations – PMH

Table 7 from AREVA, 2015c: Deep water and Nearshore/Shallow-Water Model Comparison – PMWS

Point		Offshore coupled SWAN+ADCIRC Model	Nearshore/Shallow-Water SWAN Model	Difference (Offshore - Nearshore)	Percent Difference
V1	Peak Significant Wave Height (feet)	23.0	21.6	1.3	5.9
	Peak Wave Period (seconds)	15.7	15.9	-0.2	1.3
V2	Peak Significant Wave Height (feet)	19.7	19.7	0.0	0.0
	Peak Wave Period (seconds)	15.8	15.9	-0.1	0.6

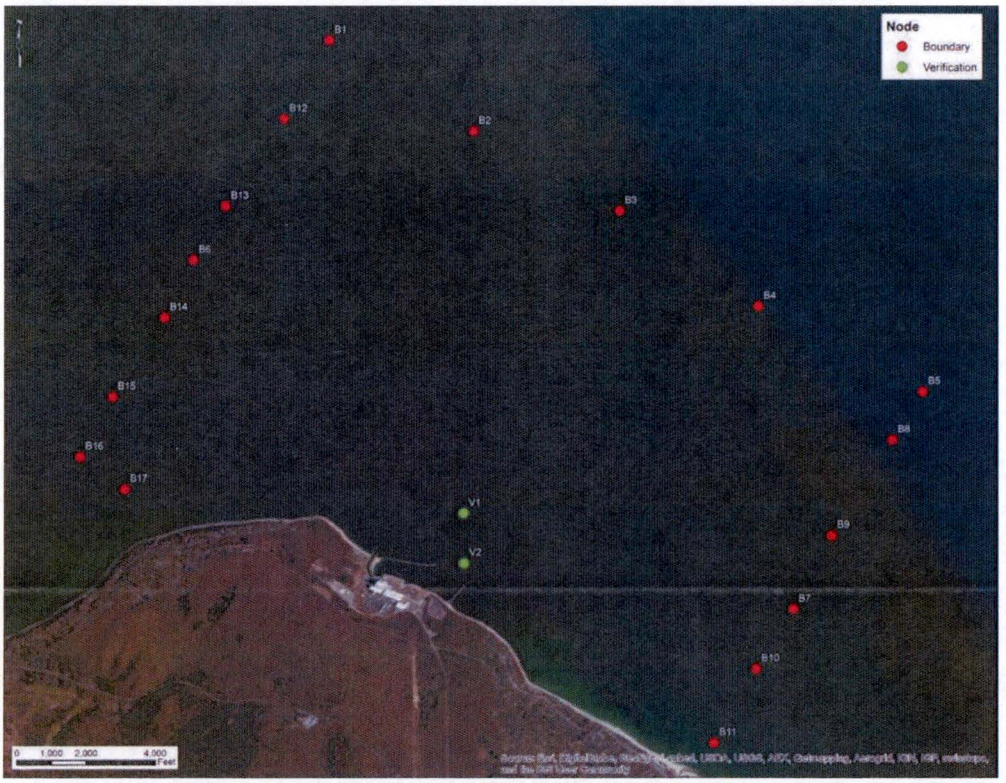

Figure 11 from AREVA, 2015c: Coupled SWAN+ADCIRC Simulation Output Locations – PMWS

In consideration of the similar wave conditions generated by the SWAN+ADCIRC model and the nearshore SWAN model, as well as the fact that initial water level conditions specified in the nearshore SWAN model were set equal to the maximum PMH/PMWS stillwater elevations outputted by the SWAN+ADCIRC model (i.e., therefore already inclusive of a measure of wave setup), it is reasonable to conclude that wave setup contributions have been conservatively considered in determining maximum flooding elevations at PNPS.

Please note: additional description of the development of and results derived from the nearshore SWAN model are presented in the Combined Event calculation (AREVA, 2015c).

Reference: AREVA, 2015c. AREVA Document No. 32-9226937-000. Pilgrim Nuclear Power Station Flooding Hazard Re-Evaluation – Combined Events. 2015.

Appendix A

A Review of the Potential Effect of Extratropical Transition of Tropical Cyclones in the Estimation of the Probable Maximum Hurricane (PMH) at the Pilgrim Nuclear Power Station

Understanding and predicting the transition of a tropical cyclone into an extratropical cyclone is an important practical and scientific challenge for weather forecasters. Atlantic tropical cyclones that make the transition while moving in a northeastward or eastward direction can have a very significant impact on shipping and eventually reach northern Europe, causing considerable loss of life and damage. Tropical cyclones that make the transition over, or offshore of, the U.S. and Canada can also do unexpected damage from heavy rains and high winds far inland.

The extratropical cyclone can sometimes intensify to central pressures that are lower, and less frequently, develop winds that are stronger, than when the transition began. During typical transitions, the area of tropical storm force winds and heavy rain expands and the storm can then have an impact over much larger area than the original tropical cyclone. The forward movement of the cyclone is usually accelerated which allows farther inland penetration or cross-ocean transit and can add to the wind speeds on right-hand side of the circulation. Together with possible re-intensification following the transition, the impact of high winds and heavy rains can be felt far inland in those circumstances. The analysis and forecasting of such events is made difficult by the relatively small size and complex internal dynamics of a tropical cyclone, compared with a non-transitioning, larger extratropical cyclone for which accurate predictions of track and intensity are more readily made. In fact, the mechanisms of extratropical transition (ET) are not well-understood, with a mixture of sometimes competing and sometimes cooperating dynamic and thermodynamic processes and energy sources that occur across a very wide range of spatial and temporal scales. For historical tropical cyclones that occurred before the modern era of the upper air observing network and satellite observations, understanding the nature, extent and timing of ET of those cyclones is particularly difficult. For example, we have a much better, though still uncertain, understanding of the ET of Hurricane Sandy than the ET of the 1938 hurricane.

Nevertheless, some useful information about ET can be discerned. The vast majority of tropical cyclones that undergo extratropical transition (ET) are much weaker than their peak tropical intensity in terms of central pressure (which is more readily measured or estimated than the storm's maximum wind speed) and most are still weakening when ET begins. Because ET begins to occur at latitudes where the background wind shear is stronger and the sea surface temperatures are lower than in the tropics or subtropics, mechanisms are in place to weaken the tropical cyclone before later re-intensification of the extratropical cyclone occurs (in about 50% of the cases), usually at longitudes well east of New England. More often than not, the storm is a tropical storm or depression, not a hurricane, when the cyclone begins to draw on the baroclinic energy source of horizontal temperature contrasts (available potential energy) that can lead to re-intensification as an extratropical cyclone. The transitioned storm may develop a very low central pressure. However, the strong relationship between central pressure and maximum sustained wind speed in the tropics and subtropics is not applicable to higher latitudes where the ET has occurred. For example, an extratropical cyclone with a central pressure of 940 hPa (millibars) at 45° N has a much lower maximum wind speed than a hurricane of 940 hPa at 25° N.

With respect to the characteristics of a PMH for the Pilgrim facility, the potential importance of an ET enhancement is limited to major hurricanes (Category 3 or higher, which is based on maximum sustained surface wind speed, not central pressure) that move rapidly northward (or far less

likely, northwestward) through New England, such as the hurricane in September 1938. ET enhancement of weaker tropical cyclones is not relevant to a PMH analysis for Pilgrim, simply because ET does not transform a weaker storm into major hurricane at those latitudes. Based on the HURDAT2 data set, 36 hurricanes have entered a 200-nautical mile proximity to Pilgrim in the historical record since 1851, regardless of their direction of forward motion. Of those storms, only 15 passed west of Nantucket, with the rest offshore and heading northeastward. Of the 36, only one has increased in category. That was Alma in 1962, which briefly increased from a Category 1 to a weak Category 2 while about 100 nautical miles south of Pilgrim and moving northeastward and eventually eastward away from land.

The strongest wind speeds of a major hurricane are typically found near the inner edge of the eye wall, a concentric ring of intense convective storms that circulate rapidly around the relatively calm eye. The eye wall of a major hurricane is typically symmetric around the eye. The well-organized symmetry of convective storms in the eye wall is essential to developing and maintaining the high winds. During their life, major hurricanes usually undergo one or more eye wall replacement cycles, with the inner eye wall contracting and eroding while a second eye wall forms at a greater radius. During this replacement, the maximum wind speed is found farther from the center, but is lower than the prior maximum associated with the original and tighter eye wall. As the new eye wall contracts, the wind speed again increases, as expected from angular momentum considerations. Because of the maximum wind speed in major hurricanes is generally negatively correlated with eye radius (or diameter of the circular eye wall) and positively correlated with eye wall symmetry, the expansion of the radius of maximum wind speed and the wind field in general, and disruptions to the eye wall symmetry reduce the maximum sustained wind speed. Such structural changes occur when a typical ET begins. The eye wall is disrupted, as colder and drier air is entrained toward the storm center, and the wind field expands. Absent an acceleration of the forward movement of the hurricane due to a speed increase of the steering winds, the maximum wind speed of a major hurricane diminishes during the disruptive changes of ET.

Some examples of northeastern and mid-Atlantic U.S. hurricanes that were affected by extratropical conditions are the 1938 hurricane, Hurricane Hazel in 1954, Hurricane Hugo in 1989, and Hurricane Sandy in 2012. Again, the extent to which baroclinic energy conversions during ET may have contributed to the reduction of the dissipation rate (except possibly for Sandy) of the maximum wind speed, particularly in the earlier major hurricanes, is uncertain.

The 1938 "Long Island Express" was aptly nicknamed. The hurricane, which was a Category 5 hurricane at the latitude of Miami, was greatly accelerated in its northward motion on the front side of an extratropical trough in the jet stream, traveling at over 40 knots as it approached and crossed New England. Thus, it did not spend much time over the colder waters north of the Gulf Stream as it approached Long Island. The maximum wind speed continued to slowly diminish, not increase, even during this rapid forward acceleration. It reached the Connecticut coast as weak Category 3. It remains the strongest New England hurricane in the historical database from 1851 onward.

Hurricane Hazel made landfall near Wilmington NC as a Category 4 hurricane. Like the 1938 hurricane, it was moving very rapidly, at 40 knots. Its wind speed immediately diminished over land. But, because of its rapid movement, it was still a Category 1 hurricane over Pennsylvania, causing unexpected damage far inland, including Canada. Hurricane Hugo in 1989 was similar. It

made landfall near Charleston, SC, as a Category 4 hurricane, moved inland at 27 knots and maintained Category 1 force into North Carolina, again causing unexpected damage far inland. It appears that the common theme is the rapid movement of a major hurricane northward, maintaining its basic tropical structure, rather than intensification due to ET. The unpredicted intensity far inland resulted in unexpected damage in areas that very rarely experience wind speeds of that magnitude over a relatively large area, in contrast to severe thunderstorms that more frequently occur, but are much more geographically limited. Consequently, such hurricane events are of particular interest to meteorologists responsible for weather forecasts and warnings.

Hurricane Sandy was quite different from the aforementioned major hurricanes. Sandy only very briefly reached major hurricane status, as a minimal Category 3 storm south of Cuba. Moving northward through the Bahamas, Sandy diminished in intensity, briefly falling to tropical storm status, while moving over warm waters and coming under the influence of upper-level, extratropical circulation patterns. Meanwhile, the area of tropical storm force winds greatly expanded in geographic coverage. It rarely had a clearly defined eye and eye wall structure. At an intensity of 60 knots early on October 27, its central pressure was 968 hPa, which for a tropical cyclone would typically be associated with a strong Category 2 hurricane. North of Cuba until shortly before New Jersey landfall, Sandy fluctuated between being primarily controlled by tropical or extratropical processes and possessing contrasting structural characteristics. On October 28 Sandy recovered some tropical characteristics. Early on October 29 it re-intensified when the vertical wind shear decreased and the storm passed over the Gulf Stream at about 24 knots, after being turned northwestward by an unusual upper-level steering pattern. During this time, it briefly became a minimal Category 2 hurricane with a maximum wind speed of 85 knots. One recent high-resolution modeling study of the re-intensification suggested the very unusual northwestward movement over the Gulf Stream allowed for an axisymmetric reinforcement of the cyclone's circulation via baroclinic processes. Moving beyond the Gulf Stream, Sandy essentially lost its tropical characteristics and was re-classified as "Post-Tropical Cyclone Sandy" shortly before landfall with a maximum sustained wind speed of 75 knots (Category 1).

The Emanuel model that generates a synthetic history of tropical cyclones does not attempt to directly include baroclinic energy sources that contribute to the potential re-intensification of cyclones during or after transition. However, the model does include the impact of enhanced forward motion on a hurricane's maximum wind speed, simply because it accommodates for the stronger steering currents that occur at the latitudes at which ET typically occurs. It also permits a major hurricane to move more rapidly into the New England area, such that the dissipation of the storm due to the loss of its tropical energy sources does not proceed as readily as a slower moving storm. For major hurricanes, the effects of the translation speed in adding to the wind speed on the right hand side of the cyclone and minimizing its time over cold water are more likely to influence the maximum wind speed of a PMH in the Pilgrim area, than an intensification due to baroclinic energy conversions. The unique processes associated with a Sandy-like late intensification would be extremely rare for a major hurricane affecting New England, if not impossible, considering the greater distance and orientation of the Gulf Stream relative to Pilgrim.

In summary, the PMH for Pilgrim is best described as a major hurricane that is translated rapidly northward, roughly paralleling the East Coast, maximizing the time over the Gulf Stream and minimizing the amount of time that the cyclone spends over the cold waters north of the Stream. The dissipative effect of the cold water is minimized if, just before reaching New England, the

cyclone remains in a relatively narrow longitude band roughly parallel with Pilgrim's longitude. Examples of this sort of cyclone are the 1938 hurricane, Esther (1961) and Gerda (1969). According to the HURDAT2 historical data, Esther was a Category 4 hurricane as far north as Delaware. It diminished to Category 3 off the New Jersey coast and made a sharp eastward turn just south of New England, while also abruptly slowing tremendously and rapidly weakening to tropical storm intensity. Gerda moved in a north-northeast direction, paralleling the East Coast, and remained over the warm waters of the Gulf Stream to the most northern latitude of the Stream near the U.S. It first reached Category 3 intensity east of Delaware and retained that intensity to about the latitude of Long Island, while passing east of Cape Cod and eventually making landfall in extreme eastern Maine as a Category 2 hurricane moving at 44 knots. Such tropical cyclones appear to be adequately modeled in the Emanuel model for the determination of the PMH for Pilgrim.

Lee E. Branscome, Ph.D., C.C.M.
Climatological Consulting Corporation
May 18, 2016

References

Best Track Data (HURDAT2), Atlantic hurricane database, 1851-2015, updated February 17, 2016, National Hurricane Center and NOAA AOML Hurricane Research Division.

Blake, E. S., et al., 2013: Tropical Cyclone Report – Hurricane Sandy, 22 -29 October 2012. National Hurricane Center.

Elsner, J. B., and A. B. Kara, 1999: Hurricanes of the North Atlantic – Climate and Society, Oxford University Press, 488 pp.

Emanuel, K., 2005: Divine Wind – The History and Science of Hurricanes, Oxford University Press, 285 pp.

Emanuel, K., and S. Ravela, 2013: Hurricane Events Sets – Description of Methods. WindRiskTech, 19 pp.

Galarneau, T.J., Jr., C. A. Davis, and M. A. Shapiro, 2013: Intensification of Hurricane Sandy (2012) through extratropical warm core seclusion. Mon. Wea. Rev., 141, 4296-4321.

Gyakum, J.R., and J. Keller, Advances in understanding extratropical transition.

Harr, P. A., and R. L. Elsberry, 2000: Extratropical transition of tropical cyclones over the western North Pacific. Part I: Evolution of structural characteristics during the transition process. Mon. Wea. Rev., 128,

Hart, R. E., and J. L. Evans, 2001: A climatology of the extratropical transition of Atlantic tropical cyclones. J. Climate, 14, 546-564.

Jones, S., et al., 2003: The extratropical transition of tropical cyclones: Forecast challenges, current understanding, and future directions. Wea. Forecasting, 18, 1052-1092.

Jones, S., 2008: Impact of air-sea interaction on the extratropical transition of tropical cyclones. ECMWF Workshop on Ocean-Atmospheric Interactions, November 2008, Reading UK, 155-162.

Lackmann, G. M., 2015: Hurricane Sandy before 1900 and after 2100. Bull. Amer. Meteor. Soc., 96, 547-559.

Landsea, C.W., et al., 2004: The Atlantic Hurricane Database Re-analysis Project: Documentation for 1851-1910 alterations and additions to the HURDAT database. Hurricanes and Typhoons – Past, Present and Future, R.J. Murmane and K.-B. Liu, ed., Columbia University Press, 178-221.

Landsea, C. W., et al., 2014: A reanalysis of the 1931-43 Atlantic Hurricane Database. J. Climate, 27, 6093-6118.

NOAA Historical Hurricane Tracks, coast.noaa.gov/hurricanes

Saffir-Simpson Hurricane Wind Scale, National Hurricane Center

Appendix B

In each panel of Figure 1 from the PMH calculation (AREVA, 2015a), which is reproduced below, HURDAT2 data for the PNPS subregion are shown as large blue dots, while HURDAT2 data from 12 other subregions extending to the east, west, and south are displayed in small gray dots. A linear regression line based on all plotted data is shown for each parameter pair as a red line. Note that rmxw is maximum wind speed, fdir is storm bearing, and fspd is storm forward/translational speed.

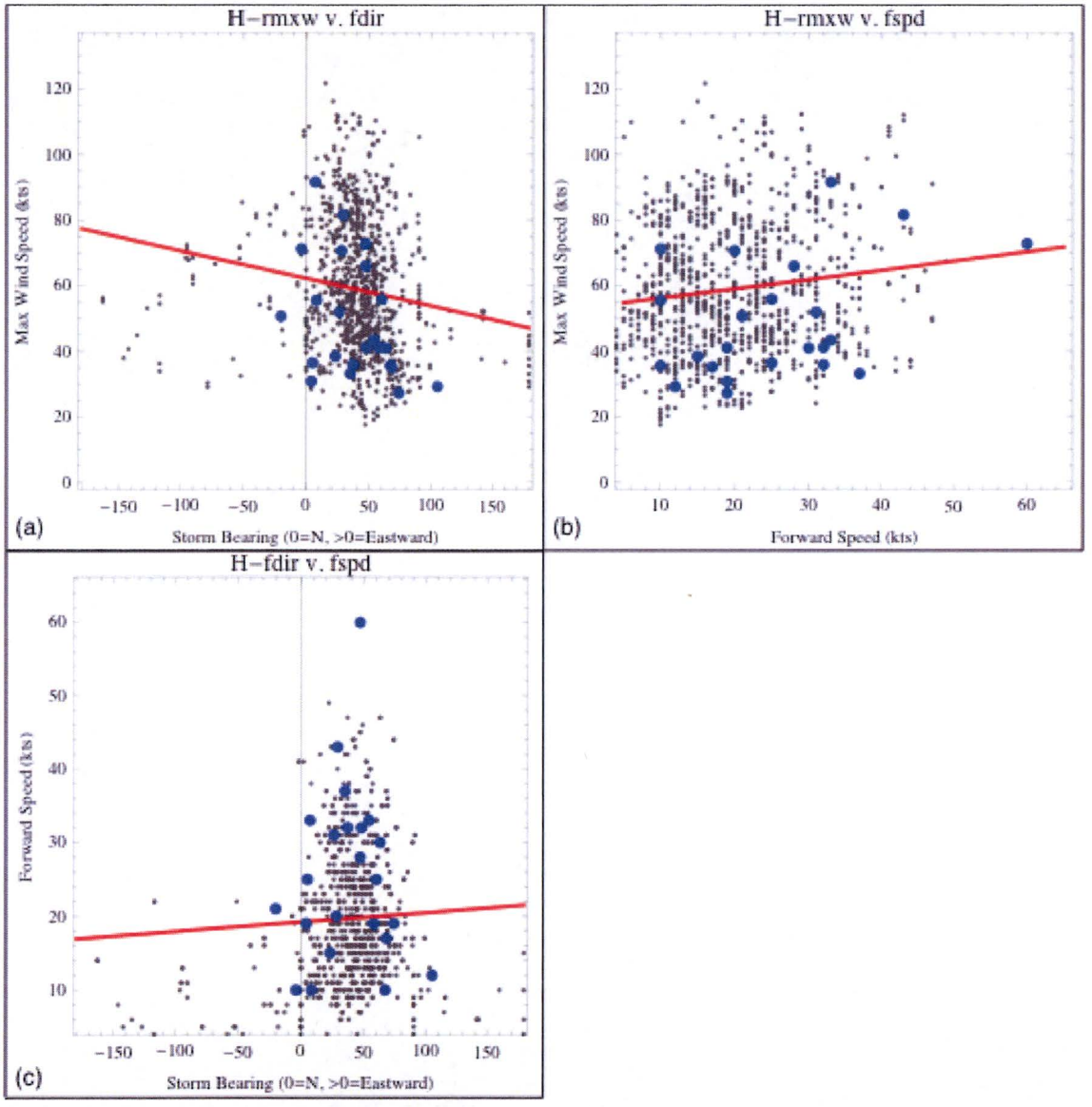

Figure 1 from AREVA, 2015a: Scatter plots of the hurricane parameter pairs: rmxw-fdir (panel a), rmxw-fspd (panel b) and fdir-fspd (panel c). Gray dots include all data within the HURDAT domain. Large blue dots are from PNPS data. The red line is a linear regression line through all data.

Panel (a) from Figure 34 shows that the strongest storms move in a north/northeast direction, with infrequent, lower intensity storms moving in other directions including west-of-north. It is important to note that the number of storms moving west-of-north does not rapidly decrease as bearing angle decreases.

As shown in Figure 2 (below), which plots parameters extracted from the synthetic WRT data set, the features of each scatter plot are consistent with the corresponding HURDAT2 counterpart (i.e., refer to Figure 1). Consistent with the characteristics shown in Figure 1, the linear regression lines for the two scatter plots with fdir as a parameter (i.e., panel (a) and panel (c)) are not representative of parameter relationships, as the dominant feature of each plot is distinctly nonlinear. Note that vm is maximum wind speed.

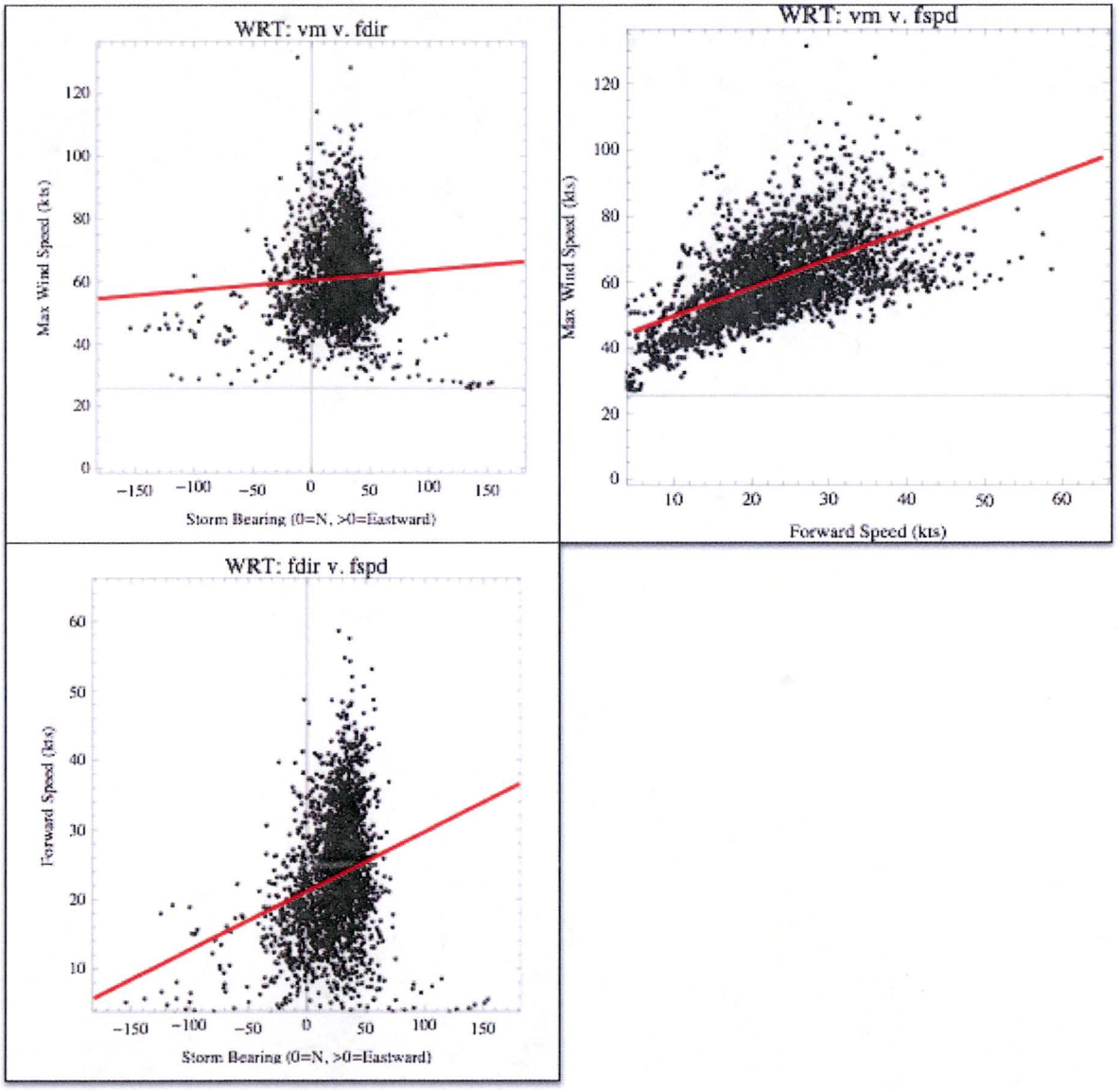

Figure 2 from AREVA, 2015a: Scatter plots of the WRT hurricane parameter pairs: vm-fdir (panel a), vm-fspd (panel b) and fdir-fspd (panel c) within the PNPS subregion. The red lines are linear regression lines through all data.

Figure 49 from the PMH calculation (AREVA, 2015a) below,Figure 3 shows the vm values, conditioned on the approach bearing sector, associated with return periods of 100, 1,000, 10,000, 100,000 , and 1,000,000 years. These return periods are derived from univariate probability density functions and reflect only consideration of the joint probability of storm bearing and storm intensity (i.e., based on maximum wind speed). The blue lines show the results with parameter co-variability included, and the red lines are results under the assumption of parameter independence. For all storms traveling west of 0˚, the parameter independence assumption does not reflect the non-linearity in the relationship between vm and fdir and therefore over-predicts storm intensities at fixed return periods.

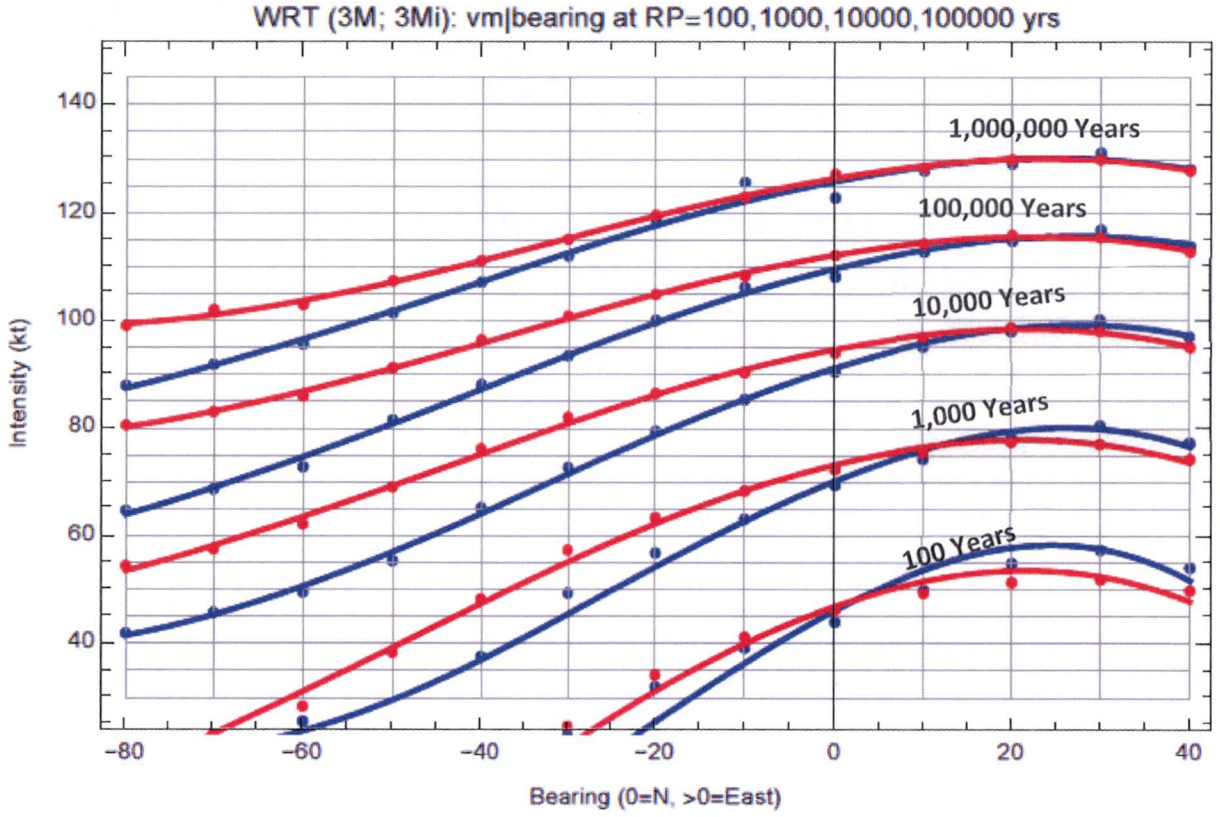

Figure 3 fraom AREVA, 2015a: Storm intensity associated with different westward approach bearings at fixed return periods of 100, 1,000, 10,000, 100,000, and 1,000,000 years. Joint parameter variability is shown in blue and independent parameter variability in red.

For equal probability levels, maximum wind speeds are greater for storms bearing slightly east-of-north (i.e., 20° to 30°) relative to other storm bearings. As bearing shifts to north and west-of-north, maximum wind speeds decrease at equal probability levels. Using Figure 3, maximum wind speeds were selected from the joint vm-fdir variability relationship, where maximum wind speed and storm bearing co-variability is recovered. Expert meteorologist judgement informed by the extreme value analysis of HURDAT2 and WRT maximum wind speed data is applied to identify the 1,000,000 year return period joint variability relationship from Figure 3 as being conservatively representative of PMH-level intensities at PNPS. This relationship provides

maximum wind speed limits ranging from 130 kt (i.e., a moderate Category 4 intensity) at a bearing of 30° to 88 kt (i.e., moderate Category 1 intensity) at a bearing of -80°.

Reference: AREVA, 2015a. AREVA Document No. 32-9226726-000. Pilgrim Nuclear Power Station Flooding Hazard Re-Evaluation – Probable Maximum Hurricane/ Probable Maximum Wind Storm. 2015.

Appendix C

Appendix C

1.0 Purpose

The purpose of this assessment is to estimate potential damage to the main breakwater structure at Pilgrim Nuclear Power Station (PNPS) occurring as a result of the Probable Maximum Hurricane (PMH) or Probable Maximum Wind Storm (PMWS). The breakwater damage is estimated herein in the form of a reduction to the top elevation of the structure. The resulting reduced elevations are used as inputs to a SWAN-based sensitivity analysis to assess wave action responses in the PNPS vicinity.

2.0 Methodology

The damage to the main breakwater during the PMH and PMWS was estimated using the Hudson formula (Reference 1). This approach estimates the armor unit stability of a breakwater structure using the formula:

$$W = \frac{\gamma_r H^3}{K_D \left(\frac{\gamma_r}{\gamma_w} - 1\right)^3 \cot\theta} \quad (1)$$

where:

W = required individual armor unit weight, *lb* (or W_{50} for graded riprap, where W_{50} is the median stone weight);

γ_r = specific weight of the armor unit, *lb/ft*^{3};

H = monochromatic (i.e., single wavelength) design wave height, *ft*;

K_D = stability coefficient, dimensionless;

γ_w = specific weight of water at the site, *lb/ft*^{3};

θ = structure slope.

The zero-damage wave height, $H_{D=0}$, is calculated by Equation (1) using the characteristic parameters of the breakwater:

$$H_{D=0} = \left(W \frac{K_D \left(\frac{\gamma_r}{\gamma_w} - 1\right)^3 \cot\theta}{\gamma_r} \right)^{\frac{1}{3}} \quad (2)$$

Using the ratio of design wave height to zero-damage wave height, $H/H_{D=0}$, the damage level in percent can be determined by Table 2-5 in Reference 1:

Table 2-5
$H/H_{D=0}$ for Cover Layer Damage Levels for Various Armor Types ($H/H_{D=0}$ for Damage Level in Percent)

Unit	$0 \le \%_D < 5$	$5 \le \%_D < 10$	$10 \le \%_D < 15$	$15 \le \%_D < 20$	$20 \le \%_D \le 30$
Quarrystone (smooth)	1.00	1.08	1.14	1.20	1.29
Quarrystone (angular)	1.00	1.08	1.19	1.27	1.37
Tetrapods	1.00	1.09	1.17	1.24	1.32
Tribars	1.00	1.11	1.25	1.36	1.50
Dolos	1.00	1.10	1.14	1.17	1.20

3.0 Analysis and Results

Assumptions

1. The armor stone of the breakwater is rough angular quarrystone, and the breakwater has two random layers of rough angular quarrystone-use structure trunk (Reference 2);
2. Individual armor unit weight: W = 12 tons or 24,000 lb (Reference 2);
3. Specific weight of armor stone: $\gamma_r = 165\ lb/ft^3$ (Reference 3);
4. The breakwater experiences the worst condition with the maximum significant wave height during the PMH/PMWS. This assumption is very conservative based on an assessment of simulated wave conditions and water levels during the PMH and PMWS (i.e., refer to Figures 2 and 3).

Design Input

1. Specific weight of sea water: $\gamma_w = 64\ lb/ft^3$;
2. The slope of the breakwater is: 2H:1V, therefore, $\cot\theta = 2$ (Reference 2).

Breakwater Damage Calculation Based on Hudson (1961)

Based on Assumption 1, Design Input 2, and Table 2-3 of Reference 1, the stability coefficient K_D=2.

Based on Equation (2), the zero-damage wave height:

$$H_{D=0} = \left(W \frac{K_D \left(\frac{\gamma_r}{\gamma_w} - 1\right)^3 \cot\theta}{\gamma_r} \right)^{\frac{1}{3}} = \left(24{,}000\ lb \frac{2\left(\frac{165\ lb/ft^3}{64\ lb/ft^3} - 1\right)^3 2}{165\ lb/ft^3} \right)^{\frac{1}{3}} = 13.2\ ft$$

The simulated water surface elevation and significant wave height during PMH and PMWS are extracted at a node in front of the main breakwater, which is shown in Figure 1. The time series are presented in Figure 2 and Figure 3. The maximum significant wave heights during PMH and PMWS are 14.7 ft and 16.8 ft, respectively.

During PMH, the ratio of maximum wave height to zero-damage wave height is:

$$\frac{H}{H_{D=0}} = \frac{14.7\ ft}{13.2\ ft} = 1.11$$

Based on Table 2-5 in Reference 1, the cover layer damage level at PNPS breakwater during PMH is 5 ≤$\%_D$ ≤10 or approximately 9% based on linear interpolation assuming the percentages reported in Table 2-5 reflect category medians.

During PMWS, the ratio of maximum wave height to zero-damage wave height is:

$$\frac{H}{H_{D=0}} = \frac{16.8\ ft}{13.2\ ft} = 1.27$$

Based on Table 2-5 in Reference 1, the cover layer damage level at PNPS breakwater during PMH is 15 ≤$\%_D$ ≤20 or approximately 18% assuming the percentages reported in Table 2-5 reflect category medians.

4.0 Conclusion

The Hudson (1961) approach was used to estimate the breakwater damage with the maximum significant wave height during the PMH and PMWS. The calculations suggest approximately 9% damage to the breakwater during the PMH and approximately 18% damage to the breakwater during the PMWS. These values should be viewed as very conservative estimates for each scenario, as model simulations suggest maximum wave heights would occur after the breakwater(s) becomes submerged. Such a condition would provide the structures with a measure of protection from damage associated with direct impacts from breaking waves. It is important to note that model simulations assumed a static antecedent water level and did not represent dynamic natural tidal fluctuations; therefore, periods of re-exposure to breaking wave conditions after initial inundation would be possible, particularly for the longer-duration PMWS scenario.

5.0 References

1. USACE, 1995. Design of Coastal Revetments, Seawalls, and Bulkheads. EM 1110-2-1614.

2. Boston Edison Company, 1979. Enclosure (1) of Response to NRC Letter. 80-66.

3. USACE, 1984. Shore Protection Manual. United States Army Coastal Engineering Research Center.

Figure 1. Location of model output node for time series of significant wave height and water level.

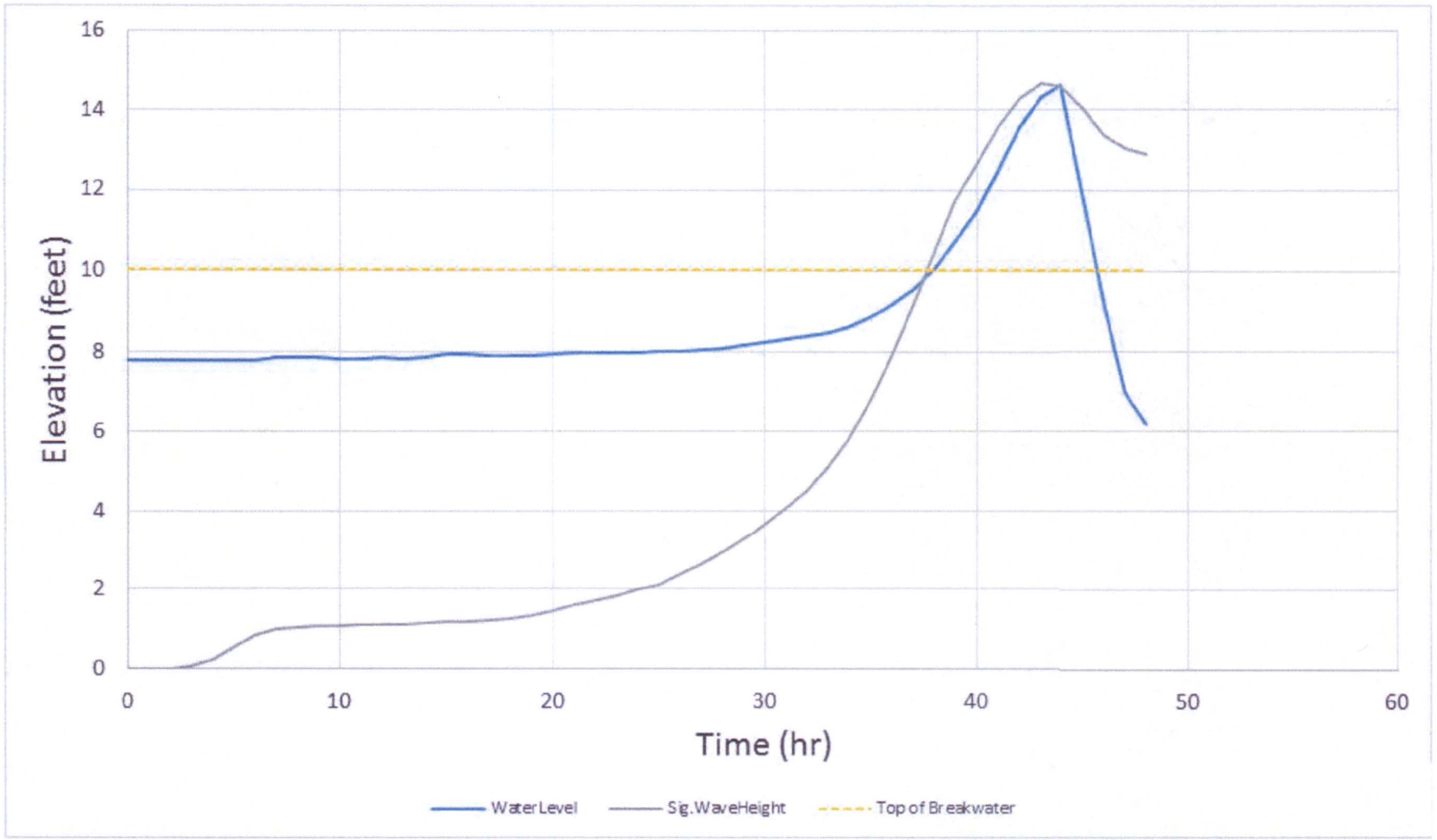

Figure 2. Water level (NAVD88) and significant wave height in front of the breakwater during PMH (refer to Figure 1).

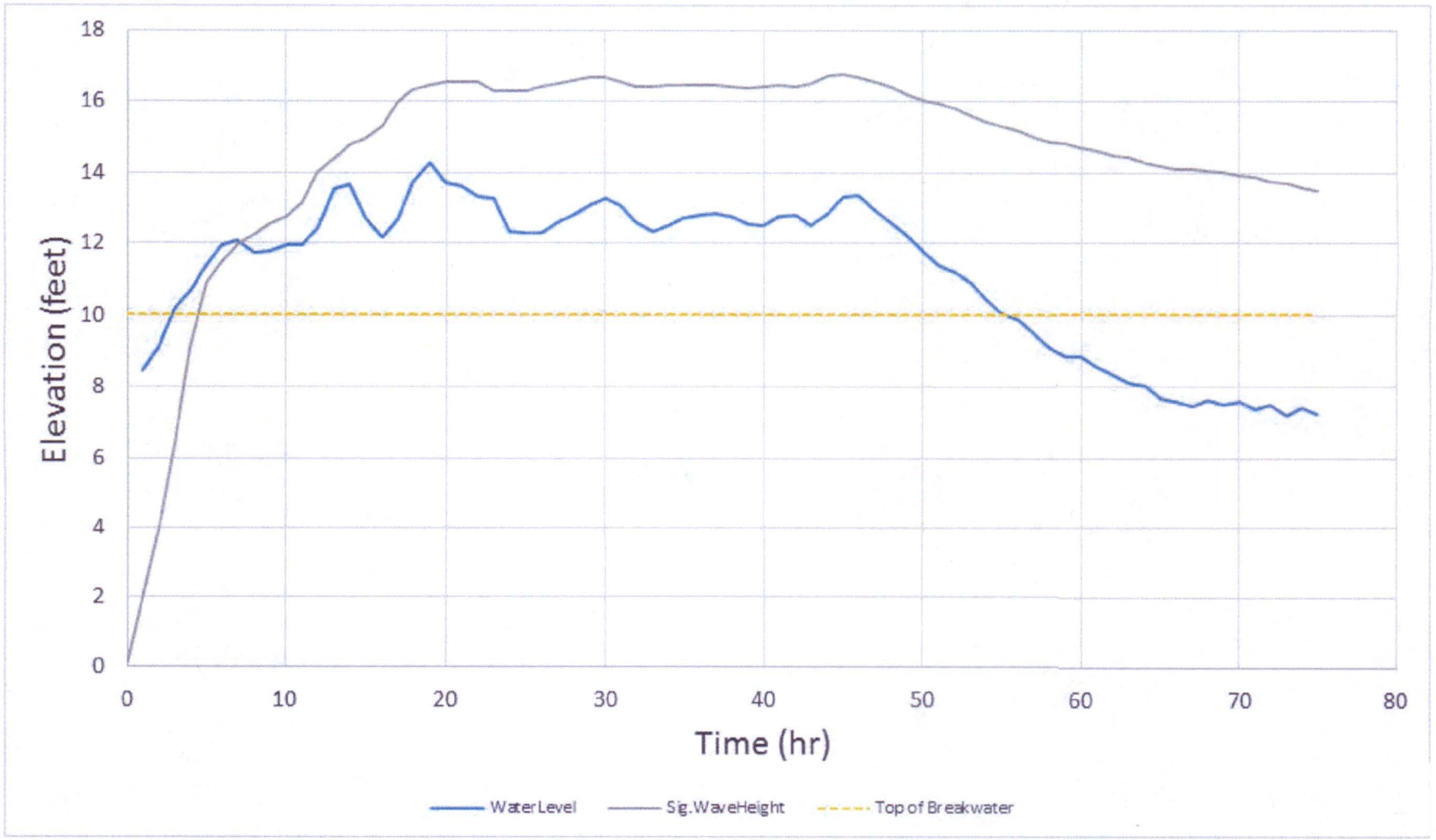

Figure 3. Water level (NAVD88) and significant wave height in front of the breakwater during PMWS (refer to Figure 1).